Available online at www.sciencedirect.com
ScienceDirect
Catalysis Today 126 (2007) 153–161
CATALYSIS TODAY
www.elsevier.com/locate/cattod

An FT-IR study of the adsorption of isopropanol on calcined layered double hydroxides containing isopolymolybdate

Daniel Carriazo, Cristina Martín, Vicente Rives *

Departamento de Química Inorgánica, Universidad de Salamanca, 37008 Salamanca, Spain

Available online 4 December 2006

Abstract

The acid–base and red–ox properties of amorphous magnesium and zinc molybdates obtained through calcination at 400 °C of Mg_2Al- and Zn_2Al-heptamolybdate layered double hydroxides, which had been prepared by anionic exchange from the corresponding nitrate-hydrotalcite precursors, have been studied. Lewis-type acid and basic sites have been detected in both systems, in addition to Brönsted-type acid sites in magnesium molybdate; however, as studied by FT-IR spectroscopy, none of them is strong enough to yield propene through isopropanol decomposition. The higher reducibility of Mo^{6+} cations in zinc-containing samples than the magnesium containing ones makes them more selective for acetone production. Moreover, a small amount of products formed on basic sites through acetone aldol reaction have been identified at high reaction temperatures.

Keywords: Hydrotalcite; Polyoxometalates; Dehydrogenation

1. Introduction

Catalytic oxidative dehydrogenation (ODH) of light alkanes has been extensively studied over vanadium [1–4] or molybdenum [5–11] based oxides (magnesium decavanadate, pyrovanadates and different molybdates of Mg, Zn, Co, Mn, etc.). It has been reported that the catalytic activities depend on many factors, such as the precise nature of the metal cation, the composition or the structure; in this way, Ueda and co-workers [5] reported that the activity of magnesium molybdate in ODH of propane to propene depends on the presence of surface MoO_x clusters which account for their acid properties. A similar behaviour in ODH of ethylbenzene to styrene was reported by Oganowski et al. [12]. Regarding dehydrogenation of propane to propene, Volta and co-workers [2] and Delmon and co-workers [3] claimed that magnesium pyrovanadate, α-$Mg_2V_2O_7$, is the most selective phase, while Kung and co-workers [1] pointed to orthovanadate, $Mg_3V_2O_8$, as the most selective one.

It has been shown that in some cases, the structure and composition of these oxide catalysts are closely related to the synthetic route followed for their preparation, since molybdenum or vanadium-based oxides might exhibit different structures depending on the polyacid precursors, which nature is strongly pH-dependent [13] in the starting aqueous solution during catalyst preparation. So this is an important factor to be taken into account when designing a catalyst.

Layered double hydroxides (LDHs), also known as hydrotalcite-type materials or anionic clays, are lamellar solids constituted by positively charged brucite-like layers, produced as consequence of a partial Mg^{2+} to Al^{3+} substitution [14,15]. This positive charge is balanced by anions located in the interlayers, which are easily exchanged by organic or inorganic anions and polar molecules. If the interlayer anion contains transition metals in a high oxidation state (i.e., as polyoxometalate, POM), mixed oxides can be prepared upon calcination of the LDHs. These mixed oxides show a larger surface area development than those prepared following conventional methods, and are active as catalysts in selective oxidation processes. It has been reported [16] that solids obtained upon calcination of decavanadate intercalated hydrotalcites are more active in propane dehydrogenation than those formed by pyrovanadate.

Catalytic decomposition of alcohols on metal oxide catalysts is one of the most important processes to produce olefins and carbonyls [17–23], via dehydration or dehydrogenation

* Corresponding author. Fax: +34 923294489.
E-mail address: vrives@usal.es (V. Rives).

0920-5861/$ – see front matter © 2006 Elsevier B.V. All rights reserved.
doi:10.1016/j.cattod.2006.10.009

processes. Several mechanisms (E_1, E_2, E_1CB) have been proposed, depending on the nature of the sites existing on the surface of the catalyst, which correspond to acid and basic sites for dehydration and basic and red–ox sites for dehydrogenation. This is the reason why decomposition of alcohols has been used as a further way to study the acid–base and red–ox properties of metal oxides catalysts [20,22]. Wachs and co-workers [24,25] have used methanol as a probe molecule to determine the concentration and nature of the surface active centres of bulk metal molybdates and vanadates, concluding that these display similar surface composition and activity toward methanol selective oxidation that supported monolayer molybdenum or vanadium oxide catalysts.

Here, we report a study on the reducibility and surface acid–base properties of systems obtained upon calcination of MgAl- and ZnAl-$Mo_7O_{24}^{6-}$ LDHs at 400 °C (temperature at which the layered structure is completely destroyed) and their activity in the adsorption and decomposition of isopropanol (ISP) in the vapour phase, aiming to correlate the reactivity and the above cited properties. The study has been carried out by FT-IR spectroscopy monitoring of the adsorption of ISP, acetic acid and acetone (possible reaction products). This technique was also applied to determine the surface acidity/basicity through adsorption of different probe molecules, such as pyridine for acid sites and trimethyl borate for basic sites.

2. Experimental

2.1. Materials

MgAl and ZnAl-heptamolybdate LDHs (hereafter denoted as MgAlMo and ZnAlMo, respectively) have been prepared by anion exchange starting from the MgAl–NO_3 and ZnAl–NO_3 LDHs, respectively, which had been synthesized following a method reported elsewhere [26,27] showing basal spacing (determined by powder X-ray diffraction, PXRD) of 8.8 and 8.9 Å, respectively. To prepare them, 50 mL of a heptamolybdate solution containing enough salt to balance the positive charge of the layers, plus a 50% in excess, were added to 100 mL of LDH-NO_3 slurries. The final pH of 4.5 was reached by the addition of a few drops of 2 M HNO_3. The mixture was kept under magnetic stirring, inert atmosphere and at 50–60 °C for 24 h, and the solids were then centrifuged, washed and dried in a desiccator under vacuum; a portion was calcined in an oven in air at 400 °C during 3 h at a heating rate of 5 °C min^{-1}, leading to samples MgAlMo400 and ZnAlMo400.

2.2. Methods

All materials were examined by powder XRD with a Siemens D-500 diffractometer using Cu Kα radiation (λ = 1.54050 Å). The samples were scanned from 5° to 70° (2θ) at a scan speed of 0.05° s^{-1} and a time constant of 1.5 s. Element chemical analysis for Mg, Al, Zn and Mo were carried out in Servicio General de Análisis Químico Aplicado (University of Salamanca, Spain) by atomic absorption in a Mark 2 ELL-240 instrument. The specific surface areas were determined by the single point method in a Micromeritics Flowsorb II 2300 instrument. Temperature programmed reduction (TPR) studies were performed in a conventional Micromeritics 2900 TPR/TPD at a heating rate of 10 °C min^{-1} and using a H_2/Ar (5 vol.%) mixture as the reducing agents (60 mL min^{-1}); these experimental conditions were chosen in order to avoid instrumental loss of resolution [28].

Surface acidity/basicity properties were determined by FT-IR monitoring of adsorption of pyridine (Py) and trimethyl borate (BATE) in a Perkin-Elmer 16PC spectrometer using self-supported discs; the sample was degassed in situ in a special cell with CaF_2 windows, at 400 °C for 2 h at 10^{-4} N m^{-2} prior to the adsorption experiments. After degassing, the probe molecule vapour was adsorbed at room temperature (rt) and the spectra recorded after degassing the samples between rt and 400 °C. The same method was used to study isopropanol (ISP) reactivity on the solids and the adsorption of acetic acid and acetone (possible products formed via ISP oxidation). In this last study, the spectra were generally recorded without outgassing the vapour phase.

3. Results and discussion

Physicochemical characterisation of these systems has been reported elsewhere [29]. The element chemical analysis results led to the following formulae: $[Mg_{0.60}Al_{0.40}(OH)_2](Mo_7O_{24})_{0.07}\cdot nH_2O$ and $[Zn_{0.67}Al_{0.33}(OH)_2](Mo_7O_{24})_{0.06}\cdot nH_2O$, for the MgAlMo and ZnAlMo samples, respectively. The PXRD patterns corresponding to the LDH precursors (Fig. 1) clearly show the diffraction peaks ascribed to planes (0 0 3), (0 0 6) and (0 0 9) at 12, 6 and 4 Å, respectively, supporting the layered hydrotalcite-type nature of these samples. From the basal spacing value (12 Å), a gallery height of 7.2 Å can be calculated, which is similar to the size calculated for the heptamolybdate anion ($Mo_7O_{24}^{6-}$) with its C_2 symmetry axis oriented perpendicularly to the brucite-like layers [30]. In addition to these peaks, other weaker diffraction lines at 10 and 5 Å are observed; the intensities of these diffraction lines increases as the formerly described peaks

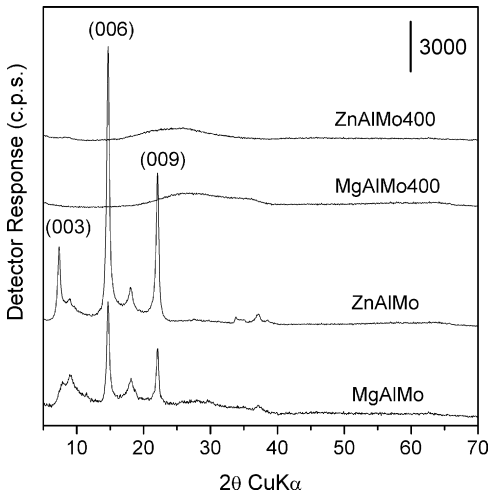

Fig. 1. PXRD patterns of as-synthesized MgAlMo and ZnAlMo samples, and calcined at 400 °C.

Table 1
Specific surface area, temperature of the reduction maximum and percentage of Mo^{6+} reduced during TPR experiments

Sample	S_{BET} ($m^2\ g^{-1}$)	T (°C)	%Mo[a]
MgAlMo	31	715	49
MgAlMo400	31	721	49
MgAlMo400 + ISP	–	715	40
ZnAlMo	28	530	89
ZnAlMo400	32	525	65
ZnAlMo400 + ISP	–	538	43

[a] Assuming that Mo^{6+} is reduced to Mo^0.

vanish when the temperature is increased above 80 °C. According to previous Raman spectroscopy results [29], these peaks at 10 and 5 Å have also been ascribed to diffraction by LDHs intercalated with heptamolybdate anions constituted by slightly distorted octahedral units [29]; this distortion would account for the decrease of the layer-to-layer distance from 12 to 10 Å. Both samples retain their hydrotalcite-type structure when calcined up to 200 °C. Calcination at 400 °C (Fig. 1) gives rise to amorphous solids (no well defined diffraction peak is observed) whose nature, according to their Raman spectra [29], corresponds to Mg–Al–Mo–O and Zn–Al–Mo–O species, containing tetrahedral and octahedral units, probably forming dimolybdate species [29]. The specific surface areas of the samples calcined at 400 °C are maintained (magnesium samples) or slightly increase (zinc samples) with respect to those measured for the uncalcined samples (Table 1).

3.1. Surface acid–base properties

3.1.1. Surface acidity

The FT-IR spectra recorded upon adsorption of Py at room temperature on the samples calcined at 400 °C, and outgassed at increasing temperatures (rt to 400 °C) are included in Fig. 2. For both samples, bands are recorded at 1606 ± 1, 1575, 1491 ± 1 and 1447 ± 1 cm^{-1}, corresponding to vibration modes 8a, 8b, 19a and 19b of Py coordinated to Lewis-type acid sites, respectively. These acid sites should only be ascribed to coordinative un-saturated (cus) Mo^{6+} ions since the bands characteristics of Py coordinated to Al^{3+} ions at 1612, 1602 and 1592 cm^{-1}, previously detected after Py adsorption on alumina or on Mg and Al amorphous oxides [31] obtained upon calcination of hydrotalcites intercalated with carbonate or nitrate, have not been detected here. The spectrum for sample MgAlMo400 also shows low intense bands at 1638 and 1538 cm^{-1} corresponding to vibration modes 8a and 19b, respectively, of protonated pyridine, which indicates that the incorporation of molybdenum species develops Brönsted acid sites, not detected for the calcined LDH precursor ($MgAl–NO_3$) [31]. The fact that Py bands are recorded for both systems even after outgassing at 300 °C indicates the high strength of these acid sites.

3.1.2. Surface basicity

The probe molecule selected has been trimethyl borate (BATE) which shows in its FT-IR spectrum very sharp bands at 1485, 1360 and 1063 cm^{-1} [32] ascribed to the deformation mode of the methyl groups and to the B–O and C–O stretching modes, respectively; these last two ones are more sensitive to interaction of BATE with surface basic sites [32].

The spectra recorded upon adsorption of BATE at room temperature on samples MgAlMo400 and ZnAlMo400, and outgassed at rt, are shown in Fig. 3. The band due to the deformation mode of the methyl groups is recorded almost in the same position as for gaseous BATE, at 1492 cm^{-1}. However, the bands due to the stretching modes of B–O and C–O bonds split into two bands each for sample MgAlMo400, and are recorded at 1391 and 1270 cm^{-1}, and at 1100 and 1074 cm^{-1}, respectively. Only the first band splits for sample ZnAlMo400 into two bands at 1378 and 1288 cm^{-1}, while that

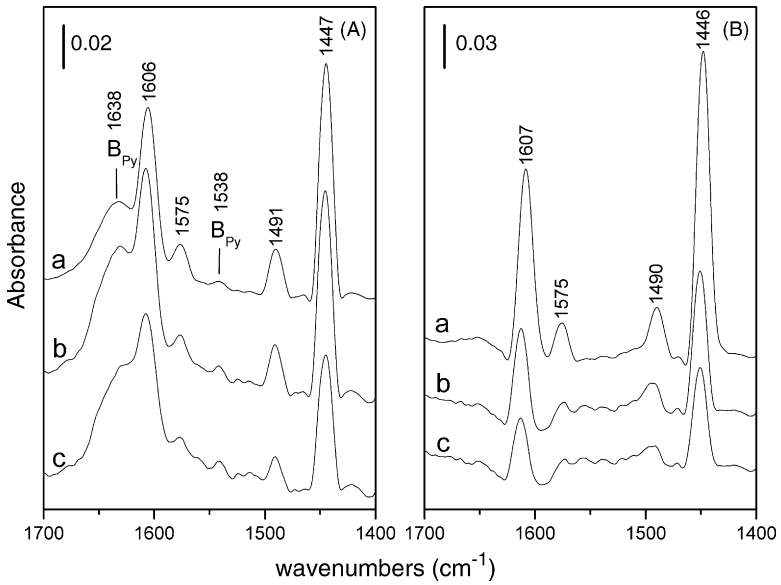

Fig. 2. FT-IR spectra recorded after Py adsorption at room temperature (rt) on samples: (A) MgAlMo400 and (B) ZnAlMo400, and outgassed at different temperatures: (a) rt (b) 200 °C and (c) 300 °C. B_{Py}: bands due to pyridine bonded to Brönsted-type acid sites.

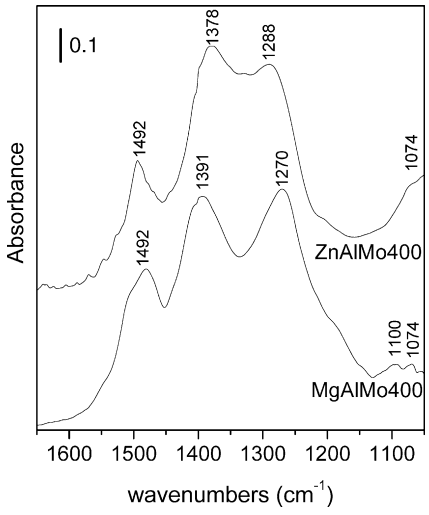

Fig. 3. FT-IR spectra recorded after adsorption of BATE at room temperature on samples MgAlMo400 and ZnAlMo400 and outgassed at rt.

due to ν(C–O) is recorded as a single band at 1074 cm^{-1}. These changes are a consequence of the strong interaction of BATE with surface Lewis basic sites (oxide and hydroxyl surface groups) giving rise to a distortion of the BATE molecule from D_{3h} to C_{3v} symmetry.

3.1.3. Red–ox properties

Temperature programmed reduction profiles for the original samples (MgAlMo and ZnAlMo) and those calcined at 400 °C are included in Fig. 4. The TPR curves for the samples calcined and treated with isopropanol (ISP) at 300 °C in situ are also included in this figure. The aim is to check if the Mo^{6+} species exposed on the surface have become partially reduced after interaction with ISP at this temperature and consequently the amount of hydrogen consumed during the TPR experiments is lower than before interaction with ISP.

In all cases, a single reduction maxima is recorded, although it is rather asymmetric. The maximum reduction rate is recorded at 715 °C for original and calcined MgAlMo sample, while for the ZnAlMo samples the maximum is recorded around 535 °C. Tetrahedral [MoO_4] units, as those existing in Na_2MoO_4, are reduced around 900 °C, while octahedral [MoO_6] species (e.g., MoO_3) are reduced around 760 or at 450–550 °C if they are dispersed. When both tetrahedral and octahedral species exist (e.g., polymeric sodium dimolybdate) intermediate reduction temperatures (767 and 677 °C) are observed [33]. In our case, although the molybdenum species existing in both systems are similar (according to their Raman spectra [29]), heptamolybdates together with a few tetrahedral molybdates ions (uncalcined samples) or amorphous dimolybdates (calcined samples), their reducibilities are quite different, as the Mg containing samples are reduced at much higher temperatures (almost 200 °C) than the zinc containing ones for which the maximum is recorded in a close position to that at which dispersed polymolybdates are reduced [34].

Consumption of hydrogen in these TPR experiments correspond exclusively to reduction of Mo^{6+} since under the experimental conditions used none of the other metallic ions are reduced (Mg, Al and Zn). Partial reduction of Zn^{2+} has been reported in some Zn containing hydrotalcites [35], but only when it is present as ZnO or this is formed during calcination; under the reduction condition used for recording the TPR curves this species is transformed into non-stochiometric oxides, $Zn_{1+x}O$. But ZnO has not been detected in our samples (ZnAlMo and ZnAlMo400), due to the low pH at which the syntheses were performed; in addition, reported Zn^{2+} reduction takes place at much higher temperatures (around 600 °C) than that here recorded.

The calculated reduction percentages for these samples are included in Table 1 considering that all the Mo^{6+} is reduced to the zero-valent state. Unfortunately, we have not been able to

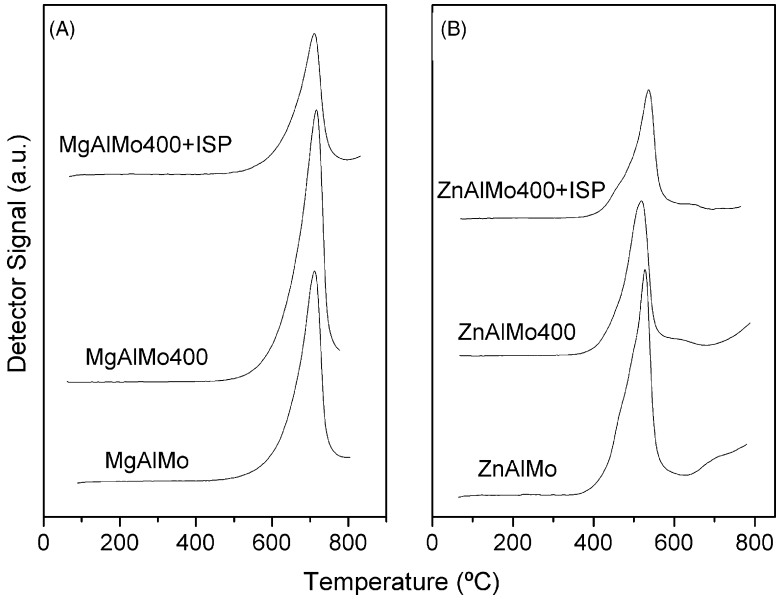

Fig. 4. TPR profiles of samples (A) MgAlMo and (B) ZnAlMo, uncalcined, calcined at 400 °C and after exposure to ISP at 300 °C.

record XPS for these samples and so only an average oxidation state of the Mo species can be suggested from the amount of hydrogen consumed during the TPR experiments. However, it is out of any doubt that the reduction degree is larger – and takes place at a lower temperature – in the Zn-containing samples.

About 50% of molybdenum species are reduced for samples MgAlMo and MgAlMo400, but this value decreases to 40% after interaction with ISP at 300 °C, indicating that the sample was probably already reduced after interaction with ISP. The reduction percentage is very much larger for the uncalcined ZnAlMo sample (ca. 90%), but decreasing to 65% for the sample calcined at 400 °C. Also in this case, the reduction is even lower after interaction with ISP at 300 °C (43%), indicating again that for both samples the interaction with ISP at 300 °C has given rise to a partial reduction of the Mo^{6+} species.

4. Isopropanol decomposition

As oxidation of isopropanol may yield acetone and acetic acid, we have monitored by FT-IR spectroscopy the adsorption of these two products (in addition to that of isopropanol) to insight in the mechanism of the reaction on our catalysts.

4.1. Adsorption of acetic acid

The spectrum recorded on contacting acetic acid vapour with sample MgAlMo400 at room temperature, shows bands at 1775, 1729, 1634, 1583, 1462, 1424, 1340, 1294 and 1178 cm^{-1}. Those recorded at high wavenumbers (1775 and 1729 cm^{-1}), together with that at 1294 cm^{-1}, are due to modes ν(C=O) and ν(C=O)/δ(C–OH) of weakly adsorbed molecular acetic acid (in the vapour phase, acetic acid shows these bands at 1770 and 1264 cm^{-1} [36]). When outgassing at room temperature (Fig. 5A) this specie is almost desorbed, but a new weak band develop at 1705 cm^{-1} due to molecularly adsorbed acetic acid bonded to stronger basic sites; these bands are recorded even after heating at 300 °C. The others bands, plus intense, at 1583, 1462, 1424 and 1340 cm^{-1}, correspond to modes ν_{as}(COO), ν_s(COO) + δ_{as}(CH_3) and δ_s(CH_3) of bidentate acetate species [37] coordinated to surface Lewis acid sites, formed through dissociative adsorption of the acid; their intensities are enhanced as the temperature is increased (Fig. 5A) and only these bands persist in the spectrum after outgassing at 300 °C (not shown).

Dissociative adsorption is also the predominating process when vapour acetic acid is adsorbed on ZnAlMo400. The spectrum is rather similar to that recorded when acetic acid is adsorbed on the sample containing magnesium. Bands corresponding to modes ν(C=O) and ν(CO)/δ(COH) of molecularly adsorbed acetic acid are recorded at 1796, 1778, 1730, 1694 and 1305 cm^{-1}; these bands are almost removed after outgassing at room temperature (Fig. 5B) although are still observed upon calcination at 300 °C. The most intense bands observed at 1569, 1464, 1431 and 1344 cm^{-1} correspond to modes ν_{as}(COO), ν_s(COO) + δ_{as}(CH_3) and δ_s(CH_3) of the acetate groups; as for the magnesium-containing system, remain even after outgassing at 300 °C.

4.2. Adsorption of acetone

The spectra recorded after adsorption of acetone at room temperature on sample MgAlMo400 are shown in Fig. 6. Some bands can be distinguished at 1742, 1718, 1368, 1232 and 1215 cm^{-1}; the first two ones correspond to vibration mode ν(C=O) and the other ones to the δ(CH_3) and ν(C–C–C) modes of physisorbed acetone, or weakly bonded to Lewis-type acid sites. Upon heating at 200 °C, in addition to these bands, new ones are developed at 3090, 1640, 1605, 1445 at 1423 cm^{-1}; the

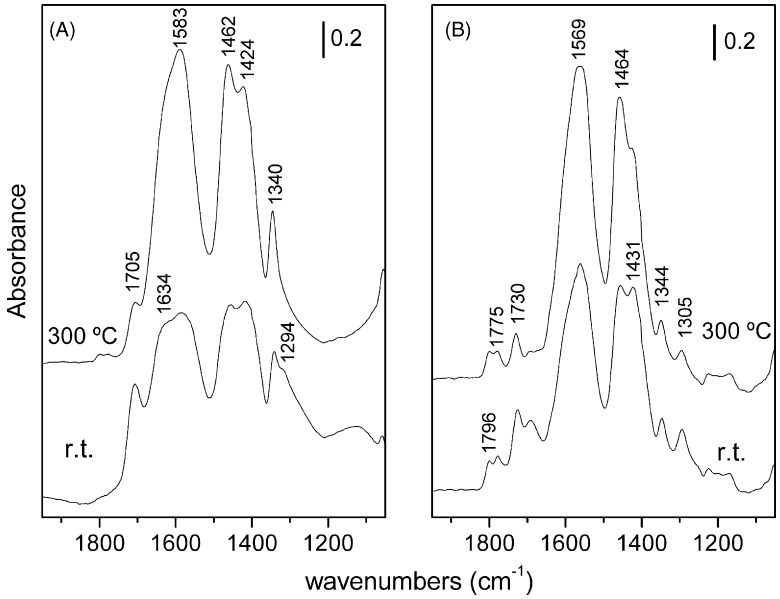

Fig. 5. FT-IR spectra recorded after adsorption of acetic acid at room temperature on samples MgAlMo400 (A) and ZnAlMo400 (B), outgassed at rt and heated at 300 °C without outgassing.

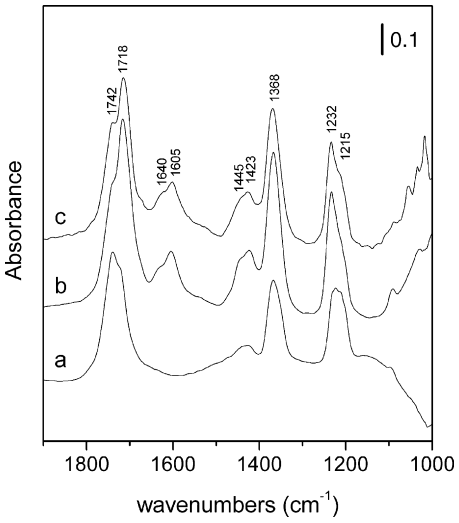

Fig. 6. FT-IR spectra recorded after adsorption of acetone at room temperature on sample MgAlMo400 (a) and heated at (b) 200 °C and (c) 300 °C.

bands at 1640 and 3090 cm^{-1} can be assigned well to the ν(CC) and ν(CH) modes of double bond units in the enol species, or well to products formed from acetone *via* aldol condensation. Figueras and co-workers [38] reported formation of diacetone alcohol and mesytil oxide as a result of gas phase acetone aldolization on meixnerite, an OH^- intercalated hydrotalcite. The bands recorded at 1605, 1445 and 1423 cm^{-1} can be assigned to modes ν_{as}(COO) and ν_s(COO) + δ_{as}(CH_3) of acetate species, since they are recorded in positions rather close, although not coincident, to those observed after adsorption of the acetic acid. This shift suggests that they probably correspond to enolate species, $^-$O–C=C/O=C–C$^-$, formed through the interaction of products from aldol condensation with surface basic sites. Formation of this sort of compounds has been previously reported by some authors when acetone is adsorbed on different metal oxides [39].

Acetone adsorption on sample ZnAlMo400 gives rise to similar spectra; in this case, the bands corresponding to the ν(C=O) and ν(C–C–C) modes of acetone split into two bands at 1742 and 1710 cm^{-1} and at 1234 and 1215 cm^{-1}, respectively; in the same way as that observed for the previous sample, the presence of bands due to the ν(C=O) mode of acetone at such high wavenumbers indicate that this molecule is physisorbed or weakly bonded on the solid surface. The bands corresponding to enol species, in this case at 1650 and 3090 cm^{-1}, are developed upon heating at 200 °C. At this temperature, enolate species are also observed, giving rise to very weak bands at 1575, 1440 and 1423 cm^{-1}.

In both cases, as acetone is merely physisorbed or weakly bonded, it is easily removed from the surface upon outgassing at rather low temperatures.

4.3. Adsorption of isopropanol

After outgassing the self-supported disc in situ for 2 h at 400 °C, as describe above, ISP was admitted to the vacuum-IR cell and the spectrum was recorded at increasing temperature without outgassing.

The spectrum recorded after adsorption of ISP at room temperature on sample MgAlMo400 (Fig. 7) shows, in the low wavenumbers region, bands at 1464, 1414, 1383, 1340, 1163, 1128 and 1112 cm^{-1}, all of them can be assigned to antisymmetric and symmetric δ(CH_3), δ(C–H), ν(C–O)/ν(C–C) and r(CH_3) modes, respectively, of isopropoxide species, formed through dissociative adsorption of the alcohol. In addition, a broad and weak band at 1295 cm^{-1}, ascribed to molecularly adsorbed ISP or hydrogen bonded to different surface basic sites, and another at 1626 cm^{-1} corresponding to δ(H–O–H) mode of water, are also recorded. All the bands mentioned remain unchanged when the sample is heated up to 250 °C. New bands at 1702 and 1240 cm^{-1} develop above 300 °C; these bands are similar to those recorded after acetone

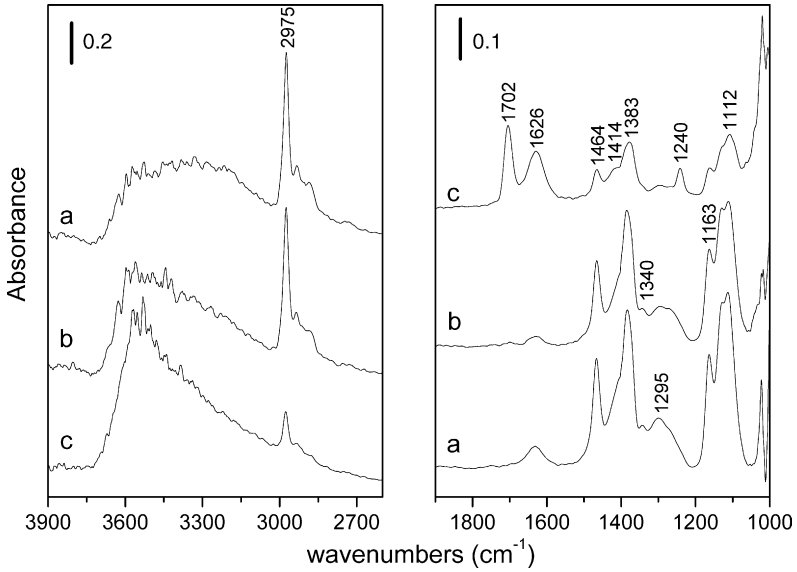

Fig. 7. FT-IR spectra recorded after adsorption of isopropanol at room temperature on sample MgAlMo400 (a) and heated at (b) 200 °C and (c) 300 °C.

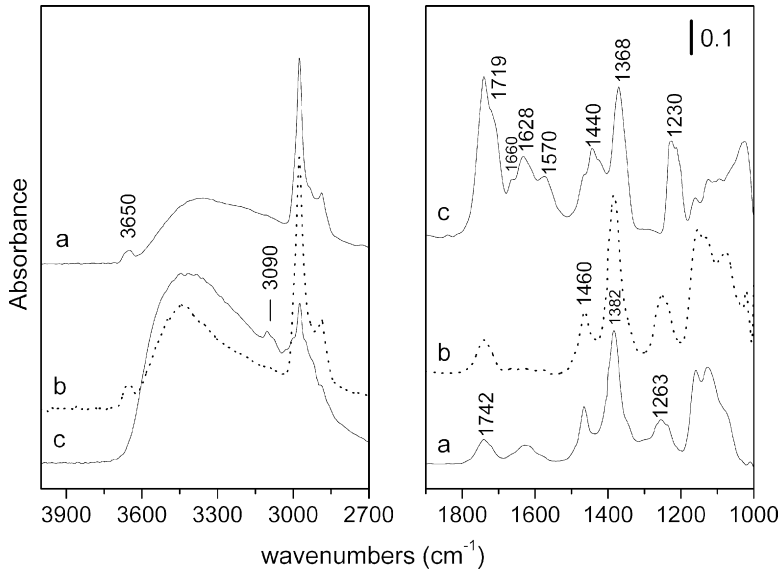

Fig. 8. FT-IR spectra recorded after adsorption of isopropanol at room temperature on sample ZnAlMo400 (a) and heated at (b) 100 °C and (c) 250 °C.

adsorption and correspond to modes ν(C=O) and ν(CCC), respectively, of acetone weakly bonded through the oxygen atom to surface Lewis-type acid centres. At this temperature (300 °C), the intensities of the bands due to alkoxide decrease, those ascribed to molecularly adsorbed ISP disappear and the band corresponding to the δ(HOH) mode of water at 1626 cm^{-1} is enhanced. Upon heating, at 400 °C only bands assigned to adsorbed acetone are enhanced. Formation of carboxylate species was not observed in any case and the bands due to adsorbed acetone disappear easily after outgassing at low temperature.

In the high wavenumbers region, it can be observed, in addition to the very intense bands between 2970 and 2890 cm^{-1} corresponding to the stretching ν(CH) mode of methyl groups of ISP, a broad band in the ν(OH) region, between 3000 and 3600 cm^{-1}, produced by different species: (1) H_2O produced through the alcohol adsorption in a dissociative way or after the acetone formation, (2) hydrogen bonded hydroxyl group of ISP molecularly adsorbed and maybe (3) new surface hydrogen-bonded hydroxyl groups.

The spectrum recorded after adsorption of ISP at room temperature on sample ZnAlMo400 (Fig. 8) shows in the low wavenumbers range the characteristic bands of isopropoxide species – similar to those described above – also the bands of molecularly adsorbed ISP or hydrogen-bonded to basic centres (1263 cm^{-1}), the band corresponding to the δ(HOH) mode of water, which in this case is recorded at 1628 cm^{-1}, and a weak band at 1742 cm^{-1} due to physisorbed acetone. In the high wavenumbers region, it can be observed, apart of the broad band between 3000 and 3600 cm^{-1} corresponding to ν(OH) of the species described in the previous paragraph and that was ascribed to the ISP methyl groups, a weak band at 3650 cm^{-1} corresponding to the ν(OH) mode of new free hydroxyl groups formed on the surface after adsorption of the alcohol. When the sample is heated at 250 °C the bands corresponding to acetone are largely enhanced; those corresponding to the ν(C=O) and ν(C–C–C) modes appear split at 1742 and 1710 cm^{-1} and at 1234 and 1215 cm^{-1}, respectively. In addition, low intense bands at 1660 and 3090 cm^{-1} are also recorded; these bands can be due to monomeric enol species or by the product formed through aldol condensation of acetone. Moreover, extremely weak bands appear at 1570, 1468 and 1440 cm^{-1}, which are ascribed to the antisymmetric and symmetric stretching modes of acetate and/or enolate species. At this temperature, the bands corresponding to the molecularly adsorbed or hydrogen-bonded ISP and to the alkoxide disappear. The spectrum is similar to that observed after adsorption of acetone at 200 °C on this same sample; almost every band coincide except that recorded at 1628 cm^{-1} which is ascribed to the δ(HOH) mode of water (absent in the acetone adsorption spectrum).

Outgassing at low temperature gives rise to desorption of all the species mentioned (i.e., the bands vanish), except those corresponding to enolate and/or acetate.

5. Final remarks

As it was mentioned above, catalytic decomposition of alcohols on metal oxides can take place following different ways: *via* dehydration to alkenes: (1) on solids possessing surface Brönsted-type centres, or *via* dehydrogenation to carbonyls; this last process can take place through simple dehydrogenation (2) over extremely basic materials without oxygen from the gas phase, or through an oxidative dehydrogenation (3) process following the Mars and van Krevelen mechanism [40], in which the presence of red–ox centres together with molecular or lattice oxygen is required.

$$CH_3{-}CHOH{-}CH_3 \rightarrow CH_2{=}CH{-}CH_3 + H_2O \quad (1)$$

$$CH_3{-}CHOH{-}CH_3 \rightarrow CH_3{-}CO{-}CH_3 + H_2 \quad (2)$$

$$CH_3{-}CHOH{-}CH_3 \rightarrow CH_3{-}CO{-}CH_3 + H_2O \quad (3)$$

The FT-IR spectra recorded indicate that ISP decomposition on both kind of samples here studied takes place through

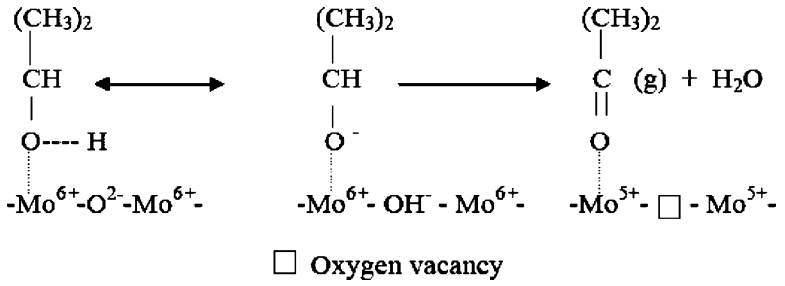

Scheme 1.

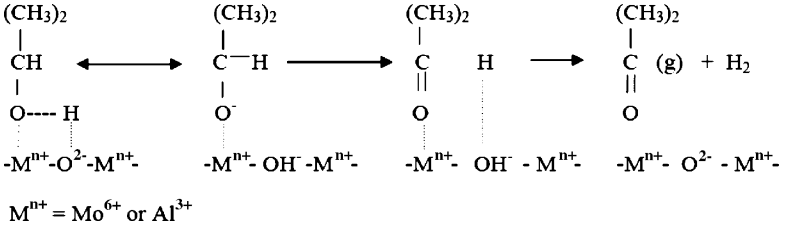

Scheme 2.

formation of the alkoxide species (isopropoxide) according to reactions:

$$(CH_3)_2CHOH + Mo^{6+}(s) + OH^-(s) \rightarrow (CH_3)_2CHO^- \cdots Mo^{6+}(s) + H_2O(g) \quad (a)$$

$$(CH_3)_2CHOH + Mo^{6+}(s) + O^{2-}(s) \rightarrow (CH_3)_2CHO^- \cdots Mo^{6+}(s) + OH^-(s) \quad (b)$$

It seems that the first reaction takes place on the Mg-containing sample, since a band corresponding to water deformation is recorded at 1626 cm^{-1}. However, both reactions would account for the results obtained when using the zinc-containing sample, since a band at 3650 cm^{-1} due to the formation of new hydroxyl groups is observed after adsorption of the alcohol.

$$(CH_3)_2CHOH \cdots OH^-(s) \rightarrow (CH_3)_2CH\text{-}O(H) \cdots HO^-(s) \quad (c)$$

$$(CH_3)_2CHOH + O^{2-}(s) \rightarrow (CH_3)_2CH{-}OH \cdots O^{2-}(s) \quad (d)$$

Molecular adsorption of the alcohol on the solid surfaces is also observed (bands at 1295 or 1263 cm^{-1}), and should take place through hydrogen bonding according to reactions (c) or (d). The band corresponding to the ν(OH) mode of the mentioned species is recorded around 3450 cm^{-1} (which is enclosed in the band registered between 3000 and 3600 cm^{-1}).

Formation of propene has not been observed along any of the tests carried out, showing the low Brönsted-type surface acidity of sample MgAlMo400. Regarding acetone production, it is larger on the Zn-containing sample, probably because of its larger reducibility and basicity. Probably, acetone is produced on both samples, MgAlMo400 and ZnAlMo400, by oxidative dehydrogenation following a Mars and Van Krevelen type red–ox process [38] (Scheme 1).

This assumption is supported by the fact that when bands due to carbonyl species appear other ones corresponding to H_2O are also recorded; moreover, the reduction percentage of Mo^{6+} species in these samples pre-treated with ISP at 300 °C (Table 1) is lower than that measured for the untreated samples, indicating that lattice oxygen takes part in dehydrogenation of ISP to acetone. However, due to the presence of strong basic sites, the production of small amounts of carbonyl compounds through simple dehydrogenation (Scheme 2) cannot be completely ruled out, especially in the case of the Zn-containing sample, on which carbonyls are formed even at room temperature.

Adsorption of ISP on the zinc-containing sample also yields aldol condensation species at 250 °C. Aldol condensation of acetone is a very interesting process from an industrial point of view, since it provides a nice route to prepare solvents, lubricants or intermediates useful for production of insecticides [41]. The process pathway is depicted in Scheme 3.

This oxide can yield isophorone, which is another product identified during gas phase aldol condensation of acetone [42].

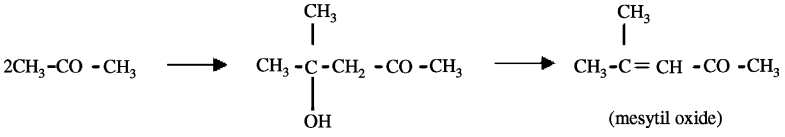

Scheme 3.

Previous studies have already proved the ability of the oxides formed upon calcination of some hydrotalcites containing Mg–Al, Ni–Al or Li–Al in the layers, with different interlayer anions (OH^-, Cl^-, NO_3^-, CO_3^{2-}, VO_4^{2-}, etc.) to behave as heterogeneous catalysts in several aldol condensation reactions [38,43–46], for which an increase in the activity is observed when the basic strength is increased. However, for condensation of benzaldehyde with acetone Rao et al. [47] have reported that the reaction rate is higher on samples outgassed at low temperatures, pointing out that hydroxyl groups are the specific basic centres responsible for aldolization; however, despite larger their basicity, only a minor reactivity of O^{2-} groups has been observed. Our results seem to be in agreement with this last claim, only on sample ZnAlMo400 a portion of acetone produced after ISP adsorption undergoes aldolic condensation, surely due to the fact that a dissociative adsorption of ISP on this sample produces new OH^- groups (detected by FT-IR spectroscopy), less basic than the O^{2-} ions, which can catalyze the aldolization reaction.

The results here reported show the effectiveness of the oxides formed upon calcination of MgAl and ZnAl-heptamolybdate hydrotalcites for acetone formation through simple or oxidative dehydrogenation of isopropanol, especially those oxides prepared from the zinc-containing system, where Mo^{6+} species are easily reduced at rather low temperatures.

Acknowledgements

Financial support from MEC (Grant MAT2003-06605-C02-01), ERDF and CONCORDE are acknowledged; D.C. acknowledges a grant from Universidad de Salamanca.

References

[1] M.A. Chaar, D. Patel, H.H. Kung, J. Catal. 109 (1988) 463.
[2] D. Siew Hew Sam, V. Soenen, J.C. Volta, J. Catal. 123 (1990) 417.
[3] X. Gao, P. Ruiz, Q. Xin, X. Guo, B. Delmon, J. Catal. 148 (1994) 56.
[4] A. Guerrero-Ruiz, I. Rodríguez-Ramos, P. Ferreira-Aparicio, J.C. Volta, Catal. Lett. 45 (1997) 113.
[5] K.H. Lee, Y.S. Yoon, W. Ueda, Y. Morooka, Catal. Lett. 46 (1997) 267.
[6] Y.S. Yoon, K. Suzuki, T. Hayakawa, S. Hamakawa, T. Shishido, K. Takehira, Catal. Lett. 59 (1999) 165.
[7] G.A. Stepanov, A.L. Tsailingol'd, V.A. Levin, F.S. Pilipenko, Stud. Surf. Sci. Catal. 7 (1981) 1293.
[8] M.C. Abello, M.F. Gómez, O. Ferretti, Appl. Catal. A: Gen. 207 (2001) 421.
[9] Y.J. Zhang, I. Rodriguez-Ramos, A. Guerrero-Ruiz, Catal. Today 61 (2000) 377.
[10] S.N. Koc, G. Gurdag, S. Geissler, M. Muhler, Ind. Eng. Chem. Res. 43 (2004) 2376.
[11] Y.F. Liu, X.P. Wang, F.P. Tian, C.Y. Jia, Chin. J. Catal. 25 (2004) 721.
[12] W. Oganowski, J. Hanuza, B. Jezouska-Trzebiatowska, J. Wrzyszcz, J. Catal. 39 (1975) 161.
[13] M.T. Pope, Heteropoly and Isopoly Oxometalates, Springer-Verlag, New York, 1983.
[14] F. Cavani, F. Trifiró, A. Vaccari, Catal. Today 11 (1991) 173.
[15] V. Rives (Ed.), Layered Double Hydroxides: Present and Future, Nova. Sci. Publ., Inc., New York, 2001.
[16] K. Bahranowski, G. Bueno, V.C. Corberan, F. Kooli, E.M. Serwicka, R.X. Valenzuela, K. Weislo, Appl. Catal. A: Gen. 185 (1999) 65.
[17] I. Wender, Catal. Rev. 26 (1984) 304.
[18] H. Knözinger, A. Scheglila, J. Catal. 14 (1970) 107.
[19] O.V. Krylov, Catalysis by Non-Metals, Academic Press, New York, 1970, p. 115.
[20] B. Grybowska-Swierkosz, Mater. Chem. Phys. 17 (1987) 21.
[21] G. Ramis, G. Busca, V. Lorenzelli, J. Chem. Soc. Faraday Trans. I 83 (1987) 1591.
[22] A. Ouqour, G. Coudurier, J.C. Vedrine, J. Chem. Soc. Faraday Trans. I 89 (1993) 3151.
[23] S.R.G. Carrazán, C. Martín, G. Solana, V. Rives, Langmuir 17 (2001) 6968.
[24] L.E. Briand, A.M. Hirt, I.E. Wachs, J. Catal. 202 (2001) 268.
[25] L.E. Briand, J.M. Jehng, L. Cornaglia, A.M. Hirt, I.E. Wachs, Catal. Today 78 (2003) 257.
[26] E. Gardner, T.J. Pinnavaia, Appl. Catal. A: Gen. 167 (1998) 65.
[27] M. del Arco, S. Gutiérrez, C. Martín, V. Rives, J. Rocha, J. Solid State Chem. 151 (2000) 272.
[28] P. Malet, A. Caballero, J. Chem. Soc. Faraday Trans. I 84 (1988) 2369.
[29] D. Carriazo, C. Domingo, C. Martín, V. Rives, Inorg. Chem. 45 (2006) 1243.
[30] Crystal Maker, Version 2.1.0, http://www.crystalmaker.co.uk/crystal-maker.
[31] M. del Arco, S. Gutiérrez, C. Martín, V. Rives, Phys. Chem. Chem. Phys. 3 (2001) 119.
[32] C. Li, Sh. Fu, H. Zhang, J. Chem. Soc., Chem. Commun. 17 (1994).
[33] I. Martín, Tesis Doctoral, Universidad de Salamanca, 1993.
[34] M. Del Arco, S.R.G. Carrazán, C. Martín, V. Rives, J. Mater. Sci. 31 (1996) 1561.
[35] C. Barriga, F. Kooli, V. Rives, M.A. Ulibarri, in: M.L. Occelli, H. Kessler (Eds.), Synthesis of Porous Materials: Zeolites, Clays, and Nanostructures, Marcel Dekker, Inc., New York, 1997, p. 661.
[36] M. Haurie, A. Novak, J. Chim. Phys. 62 (1965) 146.
[37] N.W. Alcok, V.M. Tracy, T.C. Waddington, J. Chem. Soc., Dalton Trans. (1976) 2243.
[38] R. Tessier, D. Tichit, F. Figueras, J. Kervennal, FR Patent 9500094 (1995).
[39] W.O. George, V.G. Mansell, Spectrochim. Acta 24 (1968) 145.
[40] P. Mars, D.V. van Krevelen, Chem. Eng. Sci. 3 (Suppl.) (1954) 41.
[41] B.F. Sels, D.E. De Vos, P.A. Jacobs, Catal. Rev. 43 (2001) 443.
[42] W.T. Reichle, J. Catal. 63 (1980) 295.
[43] W.T. Reichle, J. Catal. 94 (1985) 547.
[44] W. Kagunya, W. Jones, Appl. Clay Sci. 10 (1995) 95.
[45] E. Suzuki, Y. Ono, Bull. Chem. Soc. Jpn. 61 (1988) 1008.
[46] I.C. Chisem, W. Jones, C. Martín, I. Martín, V. Rives, J. Mater. Chem. 8 (1998) 1917.
[47] K.K. Rao, M. Gravelle, J. Sánchez-Valente, F. Figueras, J. Catal. 173 (1998) 115.